Beilstein-Institut
Functional Nanoscience
May 17th – 21st, 2010, Bozen, Italy

Focused Electron Beam Induced Deposition – Principles and Applications

Michael Huth

Physikalisches Institut, Goethe-Universität, Max-von-Laue-Str. 1,
60438 Frankfurt am Main, Germany

E-Mail: michael.huth@physik.uni-frankfurt.de

Received: 27th August 2010 / Published: 13th June 2011

Abstract

Focused electron beam induced deposition (FEBID) is a direct beam writing technique for nano- and micro-structures. By proper selection of the precursor gas, which is dissociated in the focus of the electron beam, different functionalities of the resulting deposits can be obtained. This contribution discusses nano-granular FEBID materials. Quite generally, nano-granular metals can be considered as tunable model systems for studying the interplay of electronic correlation effects, quantum size effects and disorder. After the introduction into the FEBID process a brief overview of the different electronic transport regimes in nano-granular metals is given. Recent experimental results on electron irradiation effects on the transport properties are presented. These results indicate a new methodology for highly miniaturized strain sensor element fabrication based on the specific electronic properties of nano-granular FEBID structures.

Introduction

Anyone who has used a scanning electron microscope (SEM) will have noticed that the area over which the electron beam is rastered for image acquisition tends to become covered with a thin film of a material which provides a rather low secondary electron yield, i. e. appears dark. This thin film, of a few nm thickness, is formed by the non-volatile electron beam induced dissociation products of hydrocarbons adsorbed on the specimen surface. The hydrocarbons themselves are part of the typical residual gas atmosphere of the SEM's

vacuum chamber. Already in 1976 this electron-beam induced dissociation phenomenon has been used for demonstrating the nano-patterning capabilities of focused electron beam induced deposition (FEBID) down to the sub-100 nm scale [1]. In the 1980s other gases were deliberately introduced in SEMs to study the results of dissociation processes with a view to obtaining deposits which might be able to provide certain functionalities, such as high metallic conductivity [2 – 4]. In the following years numerous precursor gases were systematically tested and various 2D and 3D structures were fabricated. Nevertheless, the beginning of a rather strong increase of activity in this field dates only back eight years. Since about 2002 the average number of publications and citations in the field of FEBID has increased by a factor of about 15 [5]. This can be attributed to the availability of high-resolution SEMs, often in combination with an ion-optical column for focused ion beam (FIB) processing, with commercial precursor gas injection systems. In parallel to this technological advancement FEBID, in conjunction with focused electron beam induced etching, is now routinely used in high-end tools for photolithographic mask repair in the semiconductor industry [6].

In many instances and for a large variety of precursors the structures obtained by the FEBID process are nano-granular, i. e. they are formed by a composite consisting of metallic nanocrystallites embedded in an insulating carbonaceous matrix. This has important consequences. On the one hand, the nano-granular structure leads to a significant increase of the resistivity as compared to that of the pure metal. Consequently, strong efforts are made to improve on the metal content of FEBID structures with the ultimate goal of reaching 100% pure metal deposits for a wide range of applications in mask repair and circuit editing. On the other hand, the nano-granularity influences the elastic properties of FEBID structures. Recent research has shown examples of very large hardness, approaching that of diamond, as well as rubber-like behaviour in FEBID nano-pillars depending on the precursor and process parameters [7]. And finally, the nano-granularity leads to a wealth of exciting phenomena in the electronic properties of FEBID structures. Nano-granular materials provide a model system with tunable parameters suitable for studying the interplay of electron correlations, dimensionality, and the effects of mesoscopic disorder on the electronic properties; for a recent theoretical review see [8]. From the experimental point of view the study of the electrical transport properties of nano-granular FEBID structures with particular emphasis on correlation effects has begun only recently [9, 10]. Also, it has been recognized that nano-granular materials hold some promise for strain-sensing applications [11]. This will be the topic in the last part of this manuscript which will show some very recent results of the strain-resistance effect in FEBID structures.

The FEBID Process

Figure 1 shows a schematic representation of the FEBID process. Precursor molecules, supplied close to the focal point of the electron beam by a gas injection system, are dissociated by the primary electrons, backscattered electrons and secondaries. The primary

electron beam is rastered over the substrate surface following a predefined pattern. Relevant process parameters for this raster process are the distance between successive dwell points of the electron beam (pitch) and the time period over which the electron beam is held at each dwell point (dwell time). Typical pitches vary between 10 to 100 nm. Dwell times vary much more strongly. Depending on the precursor and substrate material used, as well as the desired sample composition and targeted growth regime, the dwell time may a as short as 50 ns but can also be as long as 100 ms. A detailed recent review concerning FEBID and related techniques can be found in [12].

In the FEBID process the reaction of the electron beam with the precursor molecules adsorbed on the surface follows a second order kinetics, i. e. the reaction rate is proportional to both, the surface density of adsorbed molecules and the flux density of the electrons. From this proportionality one can conclude that all possible intermediate reactions leading to the final dissociation product (deposit and volatile components) have time scales which are short when compared to the time between two successive electron impact events. It is these intermediate reactions and processes of FEBID which are not yet investigated in sufficient detail.

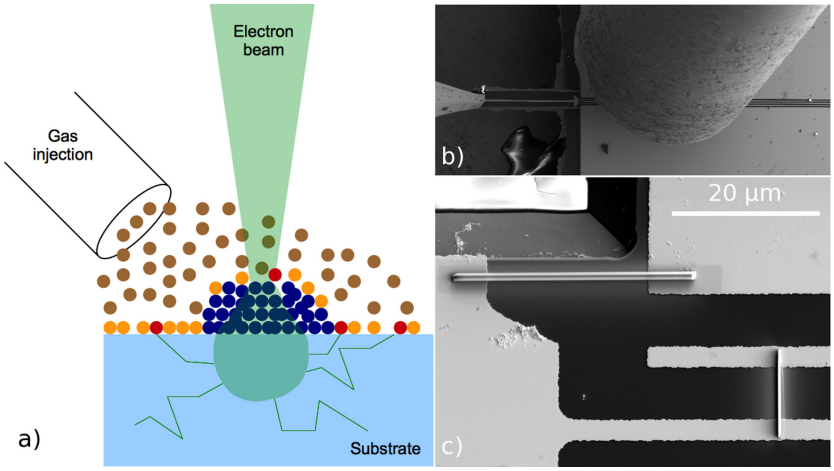

Figure 1. (a) Schematic representation of the FEBID process. The adsorbed precursor molecules (orange discs) are dissociated by electron impact (red discs) and a permanent deposit (blue discs) is formed in the focal area of the electron beam. The green lines indicate exemplary trajectories of electrons leaving the excitation volume. **(b)** SEM image of a cantilever structure with pre-defined contact lines. The gas injection capillary is visible in the upper right. On the left the W tip of a nano-manipulator is touching the cantilever. **(c)** Pt-based sensor element between contact pads (left-to-right structure) and reference element between contact pads (top-to-bottom structure) prepared by FEBID using the precursor $MeCpPt(Me)_3$.

If provided with all necessary input parameters, such as the energy-dependent dissociation cross sections and the diffusion constants for adsorbed precursor molecules, to name just two, it is possible to give a semi-quantitative account of the growth rate in FEBID on the basis of rate equation descriptions. One important ingredient in these calculations is the spatial distribution of electrons created within the Gaussian beam profile of the focussed electron beam. This distribution can be obtained from Monte Carlo simulations.

On the microscopic level there are numerous interaction mechanisms during electron impact on the precursor molecules, such as dissociation (*e.g.* by dissociated electron attachment), stimulated desorption, polymerization, and sputtering. For each of these processes an energy-dependent cross section has to be derived in order to ultimately gain more control over such aspects as purity, lateral resolution and deposition rate.

There is no theory yet that treats the FEBID process as a multi-scale problem, including microscopic and mesoscopic length scales and time scales from ultrafast (non-equilibrium processes occurring within femto seconds) to relatively slow (growth and relaxation processes requiring nanoseconds or even microseconds). First steps into tackling this multi-scale problem are currently being undertaken in the research collaboration NanoBiC funded by the Beilstein-Institut [13].

Electronic Properties of Nano-granular Metals

At large, structures prepared by FEBID fall into the class of disordered electronic materials in which disorder exists in varying degree, depending on the process parameters and the used precursor, ranging from a few impurities in an otherwise well-ordered polycrystalline host, to the strongly disordered limit of amorphous materials. In between these extremes the material can have the microstructure of a nano-granular system and is formed of reasonably well ordered nano-crystallites embedded into a carbon-rich dielectric matrix. For those FEBID structures which fall into the weak disorder limit electronic transport can be described by the scattering of Bloch waves by impurities. The theoretical framework for calculating the transport coefficients is the Boltzmann equation for the quasi-particles. For nano-granular and, naturally so, for amorphous materials it is not possible to use this conceptual framework. Disorder must be included in the theoretical analysis right from the beginning. This implies that two additional aspects must be taken into account. The first aspect is Anderson localization, which is related to the (spatial) structure of the wave function for a single electron in the presence of a random potential. The second aspect deals with interactions between electrons in the presence of this same random potential. Electron propagation for highly disordered materials is diffusive which leads to substantial modifications to the view derived from Landau's Fermi liquid theory.

From most of the electronic transport experiments on FEBID structures which can be found in the literature it becomes readily apparent that such Anderson localization effects, which are well understood in the weak-disorder limit for uncorrelated electrons, are by far dominated by much stronger effects due to the interplay of disorder and interactions. For the latter, there is no complete theoretical framework available. In this section the focus will therefore be on some new developments in the field of disordered electronic materials, and in particular, on granular electronic systems to which most of the FEBID structures can be assigned to. The compilation of recent theoretical results is not specific to materials prepared by FEBID but covers certain aspects of granular electronic metals in general. For an in-depth study of electronic transport in granular electronic systems, for which as yet no textbooks are available, the reader is referred to the recent review by Beloborodov and collaborators [8] and references therein.

Granular metals constitute one-, two- or three-dimensional arrays of (mesoscopically different) metallic particles – or grains – which are subject to an inter-granular electron coupling due to a finite tunneling probability. The arrangement of the particles, with a typical size range from a few nm to 100 nm, can be regular or irregular. For FEBID structures the tunnel coupling is provided by the carbon-rich matrix. The matrix may also contain individual metal atoms or few-atom clusters. It represents itself a disordered electronic system and can give rise to additional conductance channels due to activated transport between localized states in the matrix. This has to be taken into account for FEBID structures with a very small volume fraction of metallic particles. In most instances it can be neglected [14].

Depending on the zero-temperature limit of the electrical conductivity σ one discriminates metallic samples, showing $\sigma(T = 0) > 0$, and insulating samples, for which $\sigma(T = 0) = 0$. The effects of disorder in the grain positions and in the strength of the tunnel coupling are less important for metallic samples which are characterized by strong inter-granular coupling. For low tunnel coupling, i. e. for insulating samples, the effects of irregularities become crucial and have a direct influence on the temperature dependence of the conductivity. As a consequence of the formation processes in FEBID the obtained samples are highly disordered.

Electric transport within the metallic grains can be considered diffusive. In general, the grains will have internal defects or defects located at their surface. Trapped charges in the matrix will change the local potential of individual grains. Even if the elastic mean free path inside the grains exceeds the grain diameter, multiple scattering at the grain surface leads to chaotic motion of the electrons which is equivalent to assuming diffusive transport inside the grains due to intra-granular disorder [15]. Nevertheless, the mean spacing δ between the one-electron levels inside the grains is still a well-defined quantity. It is given by $\delta = 1/N_F V$ where $V \sim r^3$ is the grain volume and N_F denotes the density of states at the chemical potential. For grains with a diameter of a few nm, as is typically the case for FEBID

structures, δ is of the order of 1 K for metallic grains with density of states of the order of 1 $eV^{-1}nm^{-3}$. Accordingly, quantum size effects due to the discrete energy levels are only relevant at very low temperatures.

The key parameter governing most of the electronic properties of granular metals is the average tunnel conductance G between neighbouring grains. This is most conveniently expressed as a dimensionless quantity $g = G/(2e^2/h)$ by normalization to the quantum conductance. Broadly speaking, metallic behaviour will be observed, if $g \geq 1$, while samples with $g < 1$ show insulating behaviour. The normalized conductivity within a grain is denoted as g_0, not to be confused with the quantum conductance $2e^2/h$, and the notion granular metal implies that $g_0 >> g$.

Another important parameter is the single-grain Coulomb charging energy $E_C = e^2/2C$ where $C \propto r$ is the capacitance of the grain with radius r. E_C is equal to the change in electrostatic energy of the grain when one electron is added or removed. For insulating samples charge transport is suppressed at low temperatures due to this charging energy. In this respect, the insulating state is closely related to the well-known Coulomb blockade effect of a single grain connected via tunnelling to a metallic reservoir. The average level spacing can become larger than the charging energy for small grains $r < r^*$, where r^* represents the grain radius which separates the regimes for which either the condition $E_C > \delta$ or $E_C < \delta$ holds. In general, the assumption $E_C >> \delta$ is well justified for nano-granular FEBID structures.

Transport Regimes of Nano-granular Metals

The transport regimes of granular metals are classified according to the inter-grain coupling strength g. In the strong-coupling limit, $g >> 1$, a granular array has metallic properties. In the opposite regime $g << 1$ the array is insulating. The insulating state is a consequence of the strong Coulomb correlations associated with the single-electron tunnelling. The inter-grain conductance g is best considered as a phenomenological, effective parameter which controls the behaviour of the system. For FEBID structures g cannot be exactly derived from first principles for several reasons, such as the unknown grain size and coupling strength distribution and the ill-defined electronic properties of the matrix.

As temperature is reduced Coulomb correlation and interference effects become important also in the metallic regime. As a consequence, simple Drude-like relations do not hold anymore and the properties of nano-granular metals may differ considerably from those observed in homogeneously disordered metals.

Insulating regime

The insulating regime of granular systems with metallic grains is the regime to which most of the existing work on FEBID structures can be assigned to. If only nearest neighbour single-electron tunnelling is taken into account the conductivity should follow a simple Arrhenius law

$$\sigma(T) \sim \exp[-\Delta/k_B T] \tag{1}$$

as long as a hard energy gap Δ in the excitation spectrum is present at the chemical potential. Such an activated behaviour is very rarely observed in FEBID structures. Much more frequently the conductivity follows a stretched exponential temperature dependence of the form

$$\sigma(T) = \sigma_0' \exp[-(T_0/T)^{1/2}] \tag{2}$$

This functional dependence was derived by Efros and Shklovskii for doped semiconductors [16]. Until very recently it remained a puzzle why this same functional form should be obeyed by disordered granular metals in the insulating regime. An early attempt to explain this behaviour based on capacitance disorder due to the grain-size dispersion was discarded because capacitance disorder cannot fully lift the Coulomb blockade of an individual grain, so that a finite gap in the density of states at the chemical potential must remain which would necessarily lead to an Arrhenius behaviour at low temperature [17, 18]. Experimentally, the same stretched exponential was also observed in periodic arrays of quantum dots [19] and periodic granular arrays of gold particles with very small size dispersion [20]. In these systems capacitance disorder was very weak. From this arises the assumption that another type of disorder, unrelated to the grain-size dispersion, is necessary for lifting the Coulomb blockade of a single grain and can lead to a finite density of states at the chemical potential. In recent theoretical work it was suggested that electrostatic disorder, most probably caused by charged defects in the insulating matrix (or substrate), is responsible for lifting the Coulomb blockade [18]. Carrier traps in the insulating matrix at energies below the chemical potential are charged at sufficiently low temperature. They induce a potential of the order $e^2/\varepsilon r$ on the closest granule at a distance r where ε denotes the (static) dielectric constant of the matrix. For two-dimensional granular arrays one can also assume that random potentials are induced by charged defects in the substrate.

At this point it should be remarked that the simple Arrhenius behaviour can be observed in artificial, two-dimensional granular metals prepared by FEBID as detailed in [21, 22]. In these experiments the nano-granular array is formed by taking advantage of the high resolution of the FEBID process in conjunction with using a precursor, $W(CO)_6$, which tends to form near amorphous deposits that can have metal contents of about 40 at%. The diameter of

the individual amorphous grains (ca. 20 nm) leads to a well-defined Coulomb blockade which dominates the low-temperature transport properties and causes an Arrhenius behaviour of the conductivity below about 70 K.

Returning to disordered nano-granular FEBID structures it can be stated that in order to fully account for the observed stretched exponential there must be a finite probability for tunnelling to spatially remote states close to the chemical potential. This is analogous to Mott's argument in deriving his variable range hopping (VRH) law for disordered electronic systems in the non-correlated case [23]. Hopping transport over distances exceeding the average distance between adjacent granules in sufficiently dense granular arrays can in principle be realized as tunnelling via virtual electron levels in a sequence of grains, which is also called elastic and inelastic co-tunnelling. This transport mechanism was first considered by Averin and Nazarov as a means to circumvent the Coulomb blockade effect in single quantum dots [24]. In elastic co-tunnelling the charge transfer of a single electron via an intermediate virtual state in an adjacent grain to another state in a grain at a larger distance is at fixed energy. In inelastic co-tunnelling the energies of the initial state and final state differ, so that the electron leaves behind in the granule electron-hole excitations as it tunnels out of the virtual intermediate state. The intermediate states are, as the qualification *virtual* indicates, not classically accessible. The co-tunnelling mechanism was generalized to the case of multiple co-tunnelling through several grains and it was shown that the tunnelling probability falls off exponentially with the distance or the number of grains involved [20, 25, 26]. This is equivalent to the exponentially decaying probability of tunnelling between states near the chemical potential in the theory of Mott, Efros and Shklovskii for doped semiconductors [16, 27] and eventually leads to the expression given in Eq. 2. T_0 is a characteristic temperature which depends on the microscopic characteristics of the granular material in the insulating regime.

The hopping length for transport via virtual electron tunnelling decays as the temperature increases. At some temperature it will be reduced to the average grain size, so that only tunnelling to adjacent grains is possible. The variable range hopping scenario of Mott, Efros and Shklovskii no longer applies. It was suggested that the conductivity should then follow an Arrhenius behaviour [8], as has been observed in ordered granular arrays of gold particles [20] and in artificial nano-dot arrays prepared by FEBID [21, 22].

Metallic regime

As the metal content in FEBID structures increases the situation gets more complicated. In principle one can enter the regime of percolation at a critical metal volume fraction $y = y_c$ in the deposits. Such a percolating path of directly touching metallic grains can short-circuit the remaining part of sample which has activated transport behaviour. Experimentally, this can be studied by a critical exponent analysis of the dependence of the conductivity *vs.* metal

volume fraction σ(y) at the smallest accessible temperature. In order to estimate whether percolation can play a role for a given volume fraction a suitable micro-structural model has to be applied.

In recent experiments on W-based FEBID structures prepared with the precursor $W(CO)_6$ the behaviour of σ(T) shows a qualitative change from activated to non-activated behaviour as the metal content increases [10]. This is in fact indicative of a *insulator-metal transition* as a function of metal content. Apparently, the curvature of σ(T) changes sign as the metal-insulator transition is crossed. From these results it can be concluded that percolation of directly touching metallic particles is most likely not the reason for the clear change in the transport mechanism implied by the σ(T) behaviour of samples with larger metal content. It is very likely that the microstructure that forms as the metal content is increased is one in which (inelastic) tunnelling prevails to large metal concentrations because the metallic nano-crystals do not touch directly. Rather the tunnelling probability grows with metal content because of grain size growth and a reduction of the intergrain spacing. The crossover to a different transport regime is not simply percolative but is tunnelling, albeit in a more complex form which may need to take into account higher order effects in tunnelling and also correlations. Micro-structural aspects which have to be kept in mind are that the nano-crystals may often have a core-shell structure, with insulating shell, which hinders a direct percolative path to be formed.

A detailed discussion of the present theoretical understanding of the metallic transport regime of granular metals can be found in [8]. As a main result theory predicts in leading order a logarithmic temperature dependence of σ(T) independent of the dimensionality of the nano-granular metal. Experimental evidence for this was found transport measurements on annealed Pt-containing FEBID structures [9]. The possible occurrence of higher order corrections of the temperature-dependent conductivity have been discussed in [10]. New and not yet published work of the author's group on the low-temperature conductivity of electron-irradiated nano-granular FEBID structures prepared with the precursor Tri-methyl-methylcyclopentadienyl-platinum $MeCpPt(Me)_3$ give strong indications for the validity of the theoretical predictions.

Experimental Example

A particularly nice example of influence of the inter-grain coupling strength on the transport properties of Pt-based nano-granular FEBID structures prepared with the precursor $(CH_3)_3PtC_5H_4CH_3$ (Tri-methyl-methylcyclopentadienyl-platinum) is shown in Figure 2. Here, a series of identical FEBID structures has been irradiated after deposition by 5 keV electrons at 1.6 nA for different periods of time as indicated. As is evident from the plot, for increasing irradiation time the temperature-dependent conductivity shows a cross-over behaviour from thermally activated towards metallic. After several hours of irradiation this

temperature dependence has even changed towards that of a simple metal, i. e. the temperature coefficient of resistance acquires a positive sign which, one could speculate, might be a signature of beginning percolation between the Pt nano-crystallites.

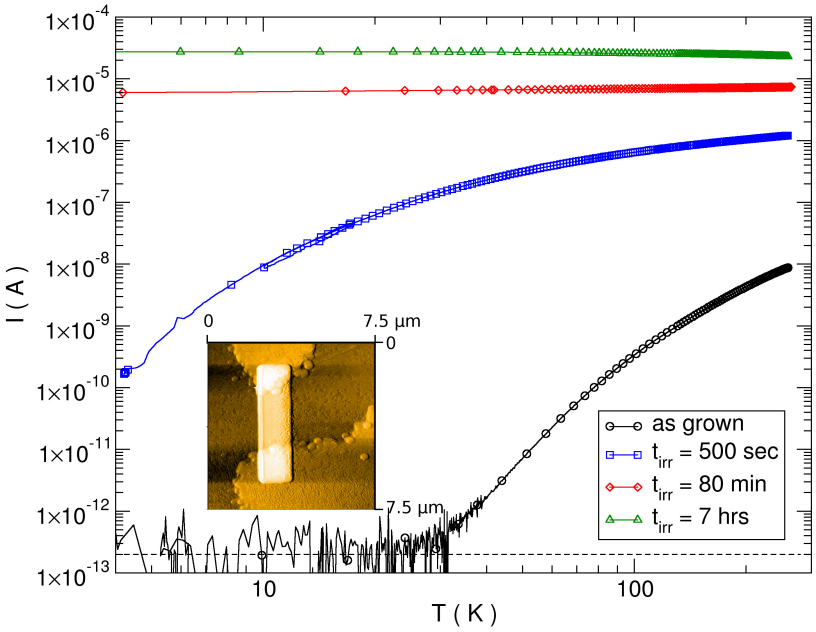

Figure 2. Temperature dependence of the current through Pt-based FEBID structures at a fixed bias voltage of 10 mV. Identical structures show strongly different temperature dependences of their conductance as they have been irradiated in a raster process for different periods of time with electrons at 5 keV and 1.6 nA current. By electron irradiation the FEBID structures can be tuned through a insulator-metal transition. The dashed line indicates the detection limit caused by the finite isolation resistance of the sample wiring. The inset shows one of the as-grown structures between two gold electrodes. The image was acquired by non-contact atomic force microscopy. Height of the deposit is about 120 nm.

Possible reasons for this dramatic change in the conductivity behaviour are irradiation-induced changes in the average Pt grain diameter and/or the properties of the dielectric function of the insulating matrix. At 5 keV beam energy the penetration depth of the electrons into the sensor material amounts to about 120 nm as can deduced from Monte Carlo simulations [28]. For deposits made with the precursor $Pt(PF_3)_4$ volume reduction by loss of phosphor and fluor in conjunction with Pt grain size growth has been reported [29]. For the precursor used in the present case recent transmission electron microscopy investigations gave no indication for a Pt grain size growth under electron irradiation [30]. Our preliminary micro-Raman experiments at 633 nm indicate a change of the dielectric matrix' vibration spectrum from amorphous to nano-crystalline but this needs further elucidation. Presently one is led to speculate that the inter-grain coupling strength growth as a conse-

quence of the electron irradiation driving a insulator-metal transition within a tunnelling-based charge transport regime. If this assumption can be further corroborated by a more detailed analysis of the micro-structural changes brought about by the irradiation process, this kind of irradiation-induced conductivity tuning in nano-granular materials would define a unique and well-controlled handle to studying the correlation-driven metal-insulator transition in disordered systems.

A quite different but innovative aspect is the application of nano-granular materials in the area of strain-sensing by strain-induced changes of the electrical resistance or conductance. Quite generally, the fact that the charge transport is dominated by tunnelling quickly leads to the conclusion that granular metals might be suitable materials for strain-sensing applications, since the tunnel coupling has an intrinsically exponential dependence on the inter-grain distance which is altered under strain; see, *e.g.*, [31] for early work or [32 – 34] for some recent work on metal-containing diamond-like carbon films.

From the standpoint of a systematic evaluation of the achievable gauge factors κ, i.e., the relative change in resistance normalized to the relative length change in the sensor,

$$\kappa = [\Delta R/R]/[\Delta L/L] \tag{3}$$

little has been done to establish an analysis scheme toward the selection of optimized material parameters which takes the advances in understanding of the charge transport mechanisms in granular metals into account. In actual fact, only recently a theoretical framework has been provided [8, 25] which appears to give full account of the phenomenological similarities in the transport properties of disordered semiconductors and granular metals. In recent work by the author a theoretical methodology for the evaluation of the intrinsic strain dependence of the electrical conductivity of nano-granular metals is introduced. It aims for providing a solid basis for estimating realistically achievable gauge factors for strain sensors based on this material class. Details of this theoretical analysis scheme, which would lead us to far astray at this point, can be found in [11]. In the following section some recent experimental work is presented which highlights some of the favourable properties of nano-granular FEBID structures for strain-sensing applications in the field of micro- and nano-electromechanical systems (MEMS, NEMS).

Application Example – Strain-resistance Effect

The field of MEMS and NEMS as enabling technology for sensor device development is rapidly progressing, due to the increasing demand for a continuous down-scaling of sensor functions in different application fields. Different approaches have been followed for nano- and microscale strain/stress measurements ranging from well-established methods, *e.g.* optical and piezoresistive (see [35, 36] and references therein), to methods still being in their infancy, *e.g.* carbon nanotubes [37] nanowires [38] and diamond-like carbon films

[39]. Here some very recent results are presented concerning a methodology for strain sensing based on nano-granular metals, using Pt-based deposits as a particularly case study [40]. A specific strength of this methodology is that it does not entail complex fabrication procedures and is readily adaptable to various sensor applications. The high resolution of the FEBID technique allows for easy down-scaling of sensor structures to below 100 nm. The gauge factor for these nano-granular metals depends on the conductivity of the sensor, which can be tuned by electron-beam irradiation leading to a distinct maximum in the sensitivity. By in situ electrical conductivity measurements we are able to tune the sensitivity of the sensor.

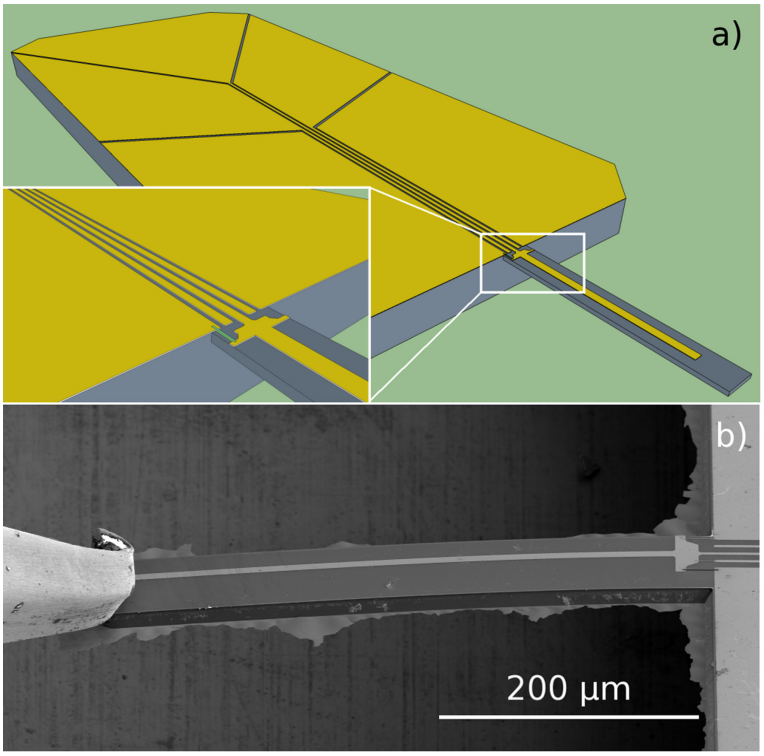

Figure 3. (a) Schematic of the cantilever structure made from silicon with Au contact pads as used in the strain-resistance effect measurements. The length of the cantilever is 500 µm, its height is 10 µm. The zoomed part indicates schematically the position of the FEBID-based strain sensor element. **(b)** SEM image of nano-manipulator tip as it touches the end of the cantilever causing it to bend. At the fixed end of the cantilever three FEBID sensor elements are visible as deposits between the electrodes.

In order to measure the sensitivity of the sensor structures deflection measurements on a cantilever template, as displayed in Figure 3, were performed. The deflection sensitivity for a rectangular cantilever beam which relates the relative resistance change $\Delta R/R$ to the cantilever deflection Δz is given by

$$\Delta R/R \cdot 1/\Delta z = 3\kappa t(l - L/2)/2l^3 \quad (4)$$

where κ is the gauge factor of the sensor element, l is the cantilever length, t is the cantilever thickness and L the sensor element length. The sensitivity of the Pt-based sensors was measured by deflecting the cantilever of the sensor chip with a closed loop nano-manipulator while measuring the relative change in resistance as a function of cantilever deflection.

As is shown in Figure 4, the sensor responds with a linear increase in resistance as the cantilever is deflected. The current-voltage characteristic is also linear (see inset) which was verified to hold true up to voltages of more than 5 V, which corresponds to an electric field of more than 2.5 kV/cm.

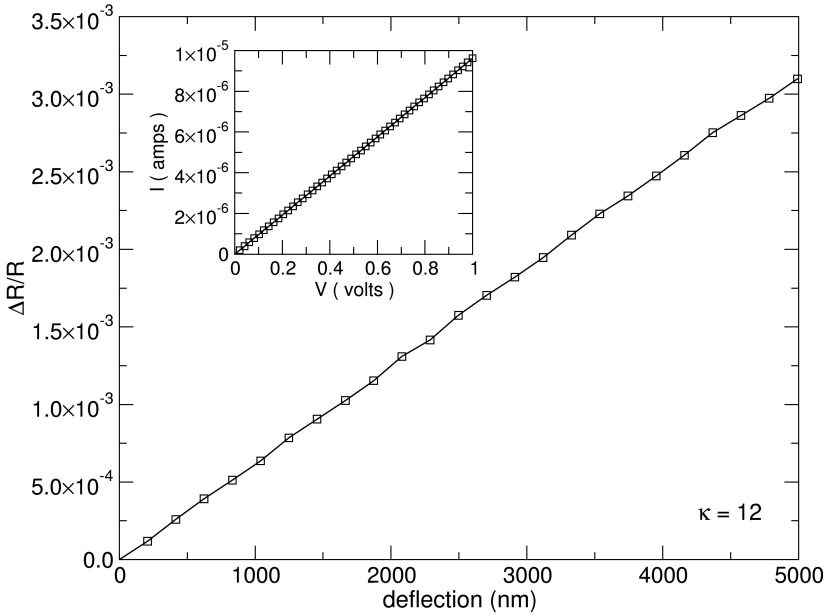

Figure 4. Relative resistance change of a Pt-based cantilever strain-sensor as the cantilever's free end is deflected by Δz. The gauge factor is 12 as indicated. The inset shows the linear current-voltage characteristics of the sensor element. Data taken at room temperature.

For the optimization of a given nano-granular material with regard to the strain-resistance effect the observed dependence of the FEBID structures' conductivity on electron irradiation provides a unique tuning capability. As one example of this effect Figure 5 shows the dependence of the gauge factor on the sensor element's resistivity as the thickness of the sensor element is increased. Apart from the resistance reduction brought about by the increase of the sensor element cross section as the thickness grows, the electron-beam

irradiation that accompanies each FEBID process does also contribute to the resistance reduction, as was discussed in the previous section. Apparently, the gauge factor exhibits a pronounced maximum corresponding to a resistance of about 75 kΩ which, assuming a homogenous deposit, amounts to a resistivity of 0.34 Ωcm. A more detailed analysis and attempt to disentangle the pure thickness from the electron irradiation effects can be found in [40].

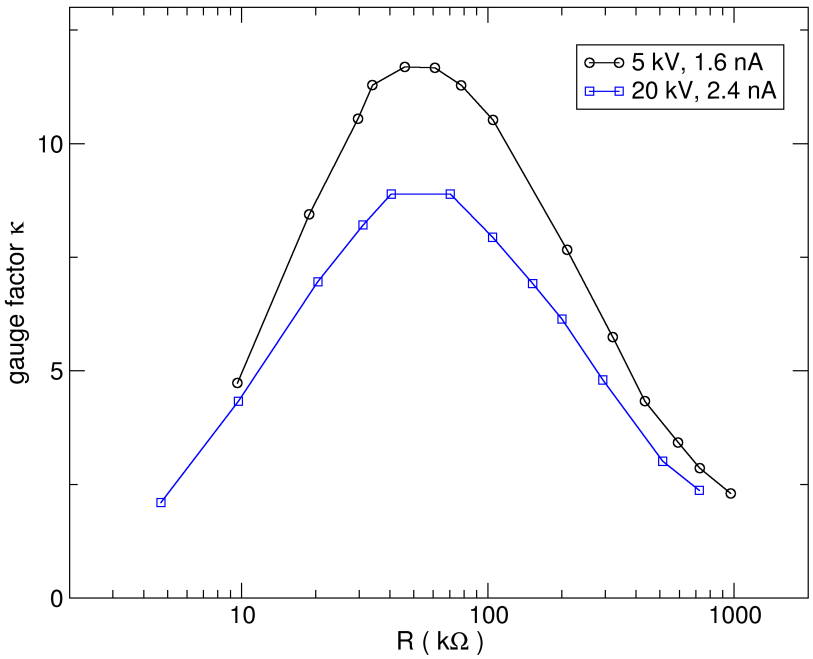

Figure 5. Gauge factor of Pt-based FEBID strain sensors fabricated at different beam conditions as indicated. The measurements were taken in the SEM using a closed-loop nano-manipulator for cantilever deflection and a Wheatstone-bridge setup in conjunction with lock-in technique for detecting the resistance change. The different sensor element resistances are obtained by increasing the thickness of the FEBID deposit. During the growth process the already formed deposit is subject to continuous electron irradiation which causes a much stronger reduction of the resistance than the the pure time-dependent increase of the deposit's height.

Conclusion

Focused electron beam deposition has developed in the last decade into a versatile technique for maskless direct beam lithography of functional nano-structures down to the sub-10 nm scale. Present disadvantages for industry-oriented application are the not yet complete control over the metal content in FEBID structures and the need for increasing the deposition yield. It may be concluded that these disadvantages are not inherent to the FEBID process

itself but rather reflect the present state of the art in precursor research. With a view to basic science, in particular the field of electronic correlation effects, FEBID does provide a novel methodology for the fabrication of (artificial) nano-granular structures with tunable properties. Recent results on the transport properties of artificial nano-dot arrays fabricated by FEBID suggest that these arrays can provide ideal experimental systems in which to study a variety of interaction-driven quantum phase transitions predicted to occur in Hubbard-like models [41] with typical energy scales in the meV regime, despite of the fact that these models have originally been developed for correlated oxides at typical energy scales of 1 eV. The usability of these correlation effects in strain-sensing applications [11, 40] is yet another aspect that indicates that future work in the field of FEBID processing will likely produce exciting and unexpected results, be it in fundamental or application-driven research.

Acknowledgments

The author acknowledges financial support by the Beilstein-Institut, Frankfurt am Main, within the research collaboration NanoBiC. Financial support by the NanoNetzwerkHessen (NNH) and by the Bundesministerium für Bildung und Forschung (BMBF) under Grant No. 0312031C is also gratefully acknowledged.

References

[1] Broers, A.N., Molzen, W.W., Cuomo, J. J. and Wittels, N.D. (1976) Electron-beam fabrication of 80 Å metal structures. *Appl. Phys. Lett.* **29**:596. doi: 10.1063/1.89155.

[2] Matsui, A. and Mori, K. (1984) New Selective Deposition Technology by Electron Beam Induced Surface Reaction. *Jpn. J. Appl. Phys., Part 2* **23**:L706. doi: 10.1143/JJAP.23.L706.

[3] Matsui, A. and Mori, K. (1986) New selective deposition technology by electron-beam induced surface reaction. *J. Vac. Sci. Technol. B* **4**:299. doi: 10.1116/1.583317.

[4] Koops, H. W.P., Weiel, R., Kern, D.P. and Baum, T.H. (1988) High-resolution electron-beam induced deposition. *J. Vac. Sci. Technol. B* **6**:477. doi: 10.1116/1.584045.

[5] Science Citation Index Expanded (SCI-EXPAND).

[6] Liang, T., Frendberg, E., Lieberman, B. and Stivers, A. (2005) Advanced photolithographic mask repair using electron beams. *J. Vac. Sci. Technol. B* **23**:3101. doi: 10.1116/1.2062428.

[7] see *e.g.* Okada, S., Mukawa, T., Kobayashi, R., Ishida, M., Ochiai, Y., Kaito, T., Matsui, S. and Fujita, J. (2006) Comparison of Young's Modulus Dependency on Beam Accelerating Voltage between Electron-Beam- and Focused Ion-Beam-Induced Chemical Vapor Deposition Pillars. *Jpn. J. Appl. Phys., Part 1* **45**:5556. doi: 10.1143/JJAP.45.5556.

[8] Beloborodov, I.S., Lopatin, A.V., Vinokur, V.M. and Efetov, K.B. (2008) Granular electronic systems. *Rev. Mod. Phys.* **79**:469. doi: 10.1103/RevModPhys.79.469.

[9] Rotkina, L., Oh, S., Eckstein, J.N. and Rotkin, S.V. (2005) Logarithmic behaviour of the conductivity of electron-beam deposited granular Pt/C nanowires. *Phys. Rev. B* **72**:233407. doi: 10.1103/PhysRevB.72.233407.

[10] Huth, M., Klingenberger, D., Grimm, Ch., Porrati, F. and Sachser, R. (2009) Conductance regimes of W-based granular metals prepared by electron beam induced deposition. *New J. Phys.* **11**:033032. doi: 10.1088/1367-2630/11/3/033032.

[11] Huth, M. (2010) Granular metals – from electronic correlations to strain-sensing applications. *J. Appl. Phys.* **107**:113709. doi: 10.1063/1.3443437.

[12] Utke, I., Hoffmann, P. and Melngailis, J. (2008) Gas-assisted focused electron and ion beam processing and fabrication. *J. Vac. Sci. Technol. B* **26**:1197. doi: 10.1116/1.2955728.

[13] see http://www.pi.physik.uni-frankfurt.de/Sonderforschungsbereich/nanobic/index.html.

[14] Porrati, F., Sachser, R. and Huth, M. (2009) The transient electrical conductivity of W-based electron-beam-induced deposits during growth, irradiation and exposure to air. *Nanotechnology* **20**:195301. doi: 10.1088/0957–4484/20/19/195301.

[15] Efetov, K. (1999) Supersymmetry in Disorder and Chaos. Cambridge University Press.

[16] Efros, A.L. and Shklovskii, B.I. (1975) Coulomb gap and low temperature conductivity of disordered systems. *J. Phys. C* **8**:L49.

[17] Pollak, M. and Adkins, C.J. (1992) Conduction in granular metals. *Philosophical Magazine B* **65**:855. doi: 10.1080/13642819208204926.

[18] Zhang, J. and Shklovskii, B.I. (2004) Density of states and conductivity of a granular metal or an array of quantum dots. *Phys. Rev. B* **70**:115317.
doi: 10.1103/PhysRevB.70.115317.

[19] Yakimov, A.I., Dvurechenskii, A.V., Nikiforov, A.I. and Bloshkin, A.A. (2003) Phononless hopping conduction in two-dimensional layers of quantum dots. *JETP Lett.* **77**:376.
doi: 10.1134/1.1581964.

[20] Tran, T.B., Beloborodov, I.S., Lin, X.M., Bigioni, T. B., Vinokur, V.M. and Jaeger, H.M. (2005) *Phys. Rev. Lett.* **95**:076806.
doi: 10.1103/PhysRevLett.95.076806.

[21] Sachser, R., Porrati, F. and Huth, M. (2009) Hard energy gap and current-path switching in ordered two-dimensional nanodot arrays prepared by focused electron-beam-induced deposition. *Phys. Rev. B* **80**:195416.
doi: 10.1103/PhysRevB.80.195416.

[22] Porrati, F., Sachser, R., Strauss, M., Andrusenko, I., Gorelik, T., Kolb, U., Bayarjargal, L., Winkler, B. and Huth, M. (2010) Artificial granularity in two-dimensional arrays of nanodots fabricated by focused-electron-beam-induced deposition. *Nanotechnology* **21**:375302.
doi: 10.1088/0957-4484/21/37/375302.

[23] Mott, N.F. (1969) Localized states in a pseudogap and near extremities of conduction and valence band. *Philosophical Magazine* **19**:835.
doi: 10.1080/14786436908216338.

[24] Averin, D.V. and Nazarov, Yu.V. (1990) Virtual electron diffusion during quantum tunnelling of the electric charge. *Phys. Rev. Lett.* **65**:2446.
doi: 10.1103/PhysRevLett.65.2446.

[25] Beloborodov, I.S., Lopatin, A.V. and Vinokur, V.M. (2005) Coulomb effects and hopping transport in granular metals. *Phys. Rev. B* **72**:125121.
doi: 10.1103/PhysRevB.72.125121.

[26] Feigelman, M.V. and Ioselevich, A.S. (2005) Variable-range co-tunnelling and conductivity of a granular metal. *JETP Lett.* **81**:277.
doi: 10.1134/1.1931015.

[27] Shklovskii, B.I. (1988) Electronic Properties of Doped Semiconductors, Springer, New York.

[28] Drouin, D., Ré al Couture, A., Joly, D., Tastet, X., Aimez, V. and Gauvin, R. (2007) CASINO V2.42 – A Fast and Easy-to-use Modelling Tool for Scanning Electron Microscopy and Microanalysis Users. *Scanning* **29**:92. doi: 10.1002/sca.20000.

[29] Botman, A., Hagen, C.W., Li, J., Thiel, B.L., Dunn, K.A., Mulders, J.J.L., Randolph, S. and Toth, M. (2009) Electron postgrowth irradiation of platinum-containing nanostructures grown by electron-beam-induced deposition from $Pt(PF_3)_4$. *J. Vac. Sci. Techn. B* **27**:2759. doi: 10.1116/1.3253551.

[30] Li, J., Toth, M., Dunn, K.A. and Thiel, B.L. (2010) Interfacial mixing and internal structure of Pt-containing nanocomposites grown by room temperature electron beam induced deposition. *J. Appl. Phys.* **107**:103540. doi: 10.1063/1.3428427.

[31] Heinrich, A., Gladun, C. and Mönch, I. (1992) Transport properties of composite thin films and application to sensors. *Int. J. Electron.* **73**:883. doi: 10.1080/00207219208925731.

[32] Takenoa, T., Miki, H. and Takagi, T. (2008) Strain sensitivity in tungsten-containing diamond-like carbon films for strain sensor applications. *Int. J. Appl. Electromagn. Mech.* **28**:211.

[33] Heckmann, U., Bandorf, R., Gerdes, H., Lübke, M., Schnabel, S. and Bräuer, G. (2009) New materials for sputtered strain gauges. *Procedia Chemistry* **1**:64. doi: 10.1016/j.proche.2009.07.016.

[34] Koppert, R., Goettel, D., Freitag-Weber, O. and Schultes, G. (2009) Nickel containing diamond like carbon thin films. *Solid State Sci.* **11**:1797. doi: 10.1016/j.solidstatesciences.2009.04.022.

[35] Zougagh, M. and Rios, A. (2009) Micro-electromechanical sensors in the analytical field. *Analyst* **134**:1274. doi: 10.1039/B901498P.

[36] Alvarez, M. and Lechuga, M. (2010) Microcantilever-based platforms as biosensing tools. *Analyst* **135**:827. doi: 10.1039/B908503N

[37] Hierold, C., Jungen, A., Stampfer, C. and Helbling, T. (2007) Nano electromechanical sensors based on carbon nanotubes. *Sens. Actuators A* **136**:51. doi: 10.1016/j.sna.2007.02.007.

[38] Zhou, J., Fei, P., Gu, Y.D., Mai, W. J., Gao, Y.F., Yang, R., Bao, G. and Wang, Z.L. (2008) Piezoelectric-Potential-Controlled Polarity-Reversible Schottky Diodes and Switches of ZnO Wires. *Nano Lett.* **8**:3973.
doi: 10.1021/nl802497e.

[39] Takeno, T., Takagi, T., Bozhko, A., Shupegin, M. and Sato, T. (2005) in Metal-containing diamond-like nanocomposite thin film for advanced temperature sensors. *Trans Tech Publications Ltd.* **475-479**:2079 – 2082.

[40] Schwalb, C.H., Grimm, C., Baranowski, M., Sachser, R., Porrati, P., Das, P., Müller, J., Reith, H., Völklein, F., Kaya, A. and Huth, M. (2010) A Tunable Strain Sensor using nanogranular metals. *Sensors* **10**:9847.
doi: 10.3390/s101109847.

[41] Stafford, C. A. and Das Sarma, S. (1994) Collective Coulomb Blockade in an Array of Quantum Dots: A Mott-Hubbard Approach. *Phys. Rev. B* **72**:3590.
doi: 10.1103/PhysRevLett.72.3590.